

Non-Affine Displacements Below Jamming under Athermal Quasi-Static Compression

Harukuni Ikeda^{1,*} and Koji Hukushima^{1,2,†}

¹*Graduate School of Arts and Sciences, The University of Tokyo 153-8902, Japan*

²*Komaba Institute for Science, The University of Tokyo, 3-8-1 Komaba, Meguro, Tokyo 153-8902, Japan*

(Dated: December 7, 2021)

Critical properties of frictionless spherical particles below jamming are studied using extensive numerical simulations, paying particular attention to the non-affine part of the displacements during the athermal quasi-static compression. It is shown that the squared norm of the non-affine displacement exhibits the power-law divergence toward the jamming transition point, and that the participation ratio of the displacements decreases near the transition point, meaning that the non-affine displacements become more localized. This can be interpreted from the development of the power-law tail of the distribution of the non-affine displacements. The critical exponents evaluated in two and three dimensions are different from each other, suggesting that the upper critical dimension below jamming is $d_{uc} > 2$, in contrast with above jamming where $d_{uc} \leq 2$.

Introduction.— When the density of constitute particles in a box is increased, the particles start to contact at a certain density, and a system suddenly acquires finite energy, mechanical pressure, and rigidity, without apparent structural changes [1]. This phenomenon called jamming has been actively studied in recent years, and the onset is defined as the jamming transition point φ_J . The jamming transition is ubiquitously observed for very diverse athermal systems such as metallic bolls [2], forms [3, 4], colloids [5], polymers [6], candies [7], dices [8], biological tissues [9], growing microbes [10] and some neural networks [11, 12].

A famous and popular numerical protocol to generate a jamming configuration is the athermal quasi-static compression (AQC), which combines the affine transformation with successive energy minimization [13]. An advantage of this protocol is that one can unambiguously define the jamming transition point φ_J as the packing fraction φ at which the energy after the minimization has a finite value. With the AQC, extensive work has been done for frictionless, spherical, and purely repulsive particles above jamming $\varphi > \varphi_J$. The numerical studies uncovered that the critical exponents do not depend on the spatial dimensions d for $d \geq 2$ [13, 14], while different values of the critical exponents are reported for a quasi-one-dimensional system [15]. The resultant critical exponents in $d \geq 2$ well agree with the mean-field predictions [16–18], suggesting that the upper critical dimension of the jamming transition is $1 < d_{uc} \leq 2$.

Somewhat surprisingly, the critical properties of the jamming transition below φ_J during the AQC have not yet been fully investigated. One of the reasons is that the quantities showing the criticality above φ_J , such as the mechanical pressure, energy, and bulk/shear modulus, are trivially zero below φ_J , and other appropriate quantities are not necessarily clear below φ_J [13]. The criticality below φ_J has been mainly investigated by adding thermal fluctuation [17, 19], introducing a moving tracer [20], considering self-propelled particles [21], or quenching from random initial configurations [22, 23]. In

particular, extensive work has been conducted on shear-driven systems [24–30]. However, it would be more desirable if one can directly extract the criticality from the configurations during the AQC, without adding thermal fluctuations and external forces. A promising study in this direction has been done by Shen *et al.* [31], where it was showed that several physical quantities, such as the displacements of the particle positions, exhibit the rapid increase just below φ_J . However, the critical exponent below φ_J and its dimensional dependence under the AQC have not been clarified yet.

In this work, we characterize the criticality below φ_J during the AQC by investigating the statistical properties of the non-affine displacements. We first report the results in $d = 3$, where the mean-squared of the non-affine displacements diverges toward φ_J with the critical exponent very close to that of the shear viscosity. By observing the participation ratio, it is shown that the displacements become more localized as the system approaches φ_J . The localization is a consequence of the development of the power-law tail of the distribution of the displacements. We also report the numerical results in $d = 2$ to discuss the dimensional dependence of the critical exponent. Our results show that the critical exponent in $d = 2$ differs from that in $d = 3$, suggesting that the upper critical dimension below φ_J is $d_{uc} > 2$, in contrast with that of above φ_J where $d_{uc} \leq 2$ [13–15].

Model.— The model mainly used in this work is frictionless spherical particles in $d = 3$. The interaction potential between N particles is given as

$$V = \sum_{i < j}^{1,N} \frac{h_{ij}^2}{2} \theta(-h_{ij}), h_{ij} = |\mathbf{r}_i - \mathbf{r}_j| - R_i - R_j, \quad (1)$$

where $\mathbf{r}_i = \{x_i, y_i, z_i\}$ and R_i respectively denote the position and radius of the i -th particle. The particles are confined in a cubic box $\mathbf{r}_i \in [0, L]^3$ with the periodic boundary conditions in all directions. To avoid crystallization, we use a binary mixture consisting of $N_S = N/2$ small particles and $N_L = N/2$ large particles. The radii

of large and small particles are $R_S = 0.5$ and $R_L = 0.7$, respectively. With those notations, the volume fraction φ is written as

$$\varphi = \frac{2\pi N(R_S^3 + R_L^3)}{3L^3}. \quad (2)$$

Numerics.— Here we describe the AQC originally proposed by O'Hern *et al.* [13]. Starting from a random initial configuration at a small packing fraction $\varphi = 0.1$, compression and energy minimization are performed successively in sequence. For each step of the compression, the packing fraction is slightly increased as $\varphi \rightarrow \varphi + \varepsilon$ with $\varepsilon = 10^{-4}$, by performing the affine transformation $\mathbf{r}_i \rightarrow \mathbf{r}_i L(\varphi + \varepsilon)/L(\varphi)$, where $L(\varphi) = [2\pi N(R_S^3 + R_L^3)/3\varphi]^{1/3}$. Then, the energy is minimized by using the FIRE algorithm, for details see Ref. [32], until the energy or squared force becomes sufficiently small: $V_N/N < 10^{-16}$ or $\sum_{i=1}^N (\nabla_i V_N)^2/N < 10^{-25}$. The procedure is repeated up to the jamming transition point φ_J at which $V_N/N > 10^{-16}$ after the minimization [13]. This algorithm determines the transition point φ_J for each sample with an accuracy of ε . After obtained φ_J , we rerun the numerical simulation with the *same* initial configuration, which allows us to calculate the physical quantities as a function of $\delta\varphi \equiv \varphi_J - \varphi$. We only use the data for $\delta\varphi \gg \varepsilon$ so that the accuracy of φ_J does not affect the results.

We perform the numerical simulations for various system sizes $N = 128, 256, 512, 1024, 2048$, and 4096 . To improve the statistic, we average over 1000 samples for $N = 128$ and 256 , and 100 samples for the other system sizes.

Mean squared displacement.— When the system is compressed from φ to $\varphi + \varepsilon$, the displacement of the i -th particle can be written as

$$\mathbf{r}_i(\varphi + \varepsilon) - \mathbf{r}_i(\varphi) = \delta\mathbf{r}_i^A + \delta\mathbf{r}_i^{\text{NA}} \quad (3)$$

where $\delta\mathbf{r}_i^A = [L(\varphi + \varepsilon)/L(\varphi) - 1] \mathbf{r}_i(\varphi)$ and $\delta\mathbf{r}_i^{\text{NA}}$ respectively denote the affine and non-affine parts of the displacement. In this work, we only focus on the non-trivial part of the displacement $\delta\mathbf{r}_i^{\text{NA}}$.

To characterize the criticality of the non-affine displacements, we first observe the mean squared displacement

$$\langle \Delta \rangle = \frac{1}{N} \sum_{i=1}^N \Delta_i, \quad (4)$$

with

$$\Delta_i = \frac{(\delta\mathbf{r}_i^{\text{NA}})^2}{3\delta l^2}, \quad (5)$$

where $\delta l = L(\varphi + \varepsilon)/L(\varphi) - 1$ accounts for the change of the linear distance L of the system. In Fig. 1 (a), we

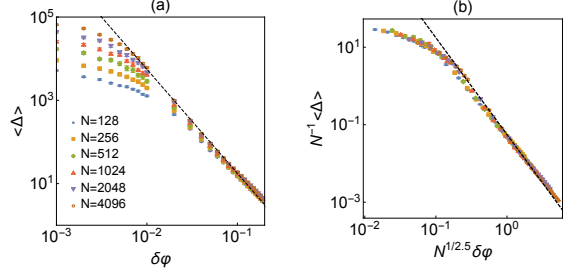


FIG. 1. (a) Mean squared non-affine displacement $\langle \Delta \rangle$ in $d = 3$. Markers denote numerical results, while the dashed line denotes the power law $\Delta \propto \delta\varphi^{-2.5}$. (b) Scaling plot of the same data.

show $\langle \Delta \rangle$ as a function of $\delta\varphi = \varphi_J - \varphi$. For large N and intermediate $\delta\varphi$, $\langle \Delta \rangle$ shows the power law

$$\langle \Delta \rangle \propto \delta\varphi^{-\beta}, \quad (6)$$

with

$$\beta = 2.5, \quad (7)$$

see the dashed line in Fig. 1 (a). A recent numerical simulation reported the similar power law for the shear viscosity η : $\eta \sim \delta\varphi^{-2.55}$ [29]. We shall discuss a possible connection between $\langle \Delta \rangle$ and η in the final section.

To further investigate the scaling of $\langle \Delta \rangle$, we perform a finite-size scaling analysis assuming the following scaling function:

$$\langle \Delta \rangle = N^\alpha \mathcal{D}(N^{\alpha/\beta} \delta\varphi), \quad (8)$$

where $\mathcal{D}(x) = O(1)$ for $x \ll 1$, and $\mathcal{D}(x) \sim x^{-\beta}$ for $x \gg 1$. As shown in Fig. 1 (b), a good scaling collapse is obtained with $\alpha = 1$. This result implies that the number of the correlated particles diverges as $N_{\text{cor}} \sim \delta\varphi^{-\beta}$, and the correlation length $L_{\text{cor}} \sim N_{\text{cor}}^{1/3} \sim \delta\varphi^{-\nu}$ with $\nu = \beta/3 = 0.83$ under the assumption that the correlated volume is compact. This is close to a previous result $\nu = 0.71$ obtained by the finite-size scaling analysis of the transition point [13].

Participation ratio.— To see the spatial structure of the displacements, we observe the normalized vector [33]:

$$\mathbf{e}_i = \frac{\delta\mathbf{r}_i^{\text{NA}}}{\sqrt{\sum_{i=1}^N (\delta\mathbf{r}_i^{\text{NA}})^2}}, \quad (9)$$

which satisfies $\sum_{i=1}^N \mathbf{e}_i \cdot \mathbf{e}_i = 1$. In Fig. 2, we visualize \mathbf{e}_i by drawing spheres such that their radii are proportional to $|\mathbf{e}_i|$. Far from jamming, the spatial distribution of \mathbf{e}_i is homogeneous and featureless, see Fig. 2 (a). On the contrary, near jamming, a few particles have very large displacements, and thus the displacement is spatially heterogeneous and localized, see Fig. 2 (d). We quantify the

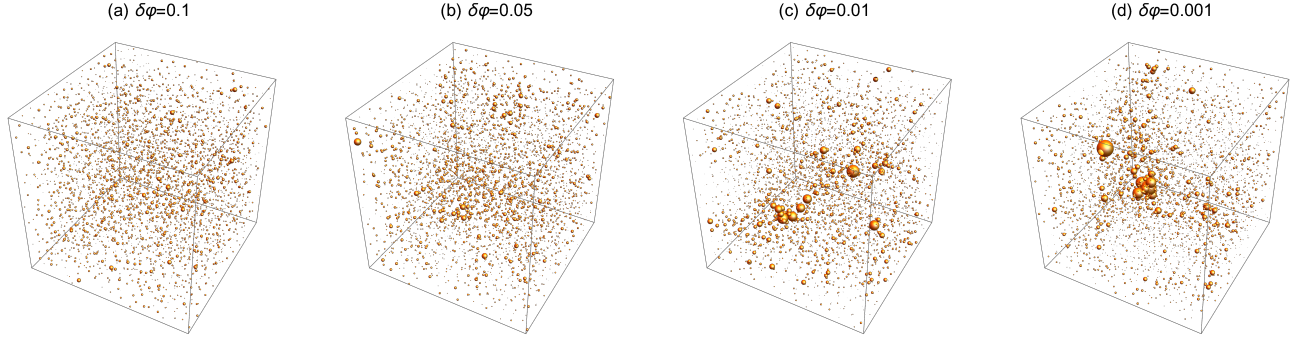


FIG. 2. Spatial distribution of non-affine displacements for $N = 4092$ particles. Diameters of spheres represent the amplitude of the (normalized) non-affine displacements $|\mathbf{e}_i|$.

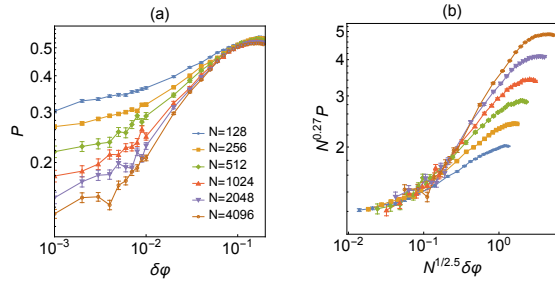


FIG. 3. (a) Participation ratio P in $d = 3$. Markers denote numerical results, and solid lines are a guide to the eye. (b) Scaling plot of the same data.

degree of the localization by using the participation ratio:

$$P = \frac{1}{N} \frac{\left(\sum_{i=1}^N \mathbf{e}_i \cdot \mathbf{e}_i \right)^2}{\sum_{i=1}^N (\mathbf{e}_i \cdot \mathbf{e}_i)^2}, \quad (10)$$

which (or inverse of which) is widely used in the study of condensed matter physics [34], including amorphous solids [35, 36]. If \mathbf{e}_i is spatially localized to a single particle, say $\mathbf{e}_i \cdot \mathbf{e}_i = \delta_{i1}$, the participation ratio P is proportional to N^{-1} . On the contrary, if \mathbf{e}_i is extended such that $\mathbf{e}_i \cdot \mathbf{e}_i \sim N^{-1}$ for all i , P is constant independent of N . In Fig. 3 (a), we show the $\delta\varphi$ dependence of P . One can see that P decreases with approaching φ_J and increasing N . To investigate the N dependence of P , we use the following scaling form:

$$P = N^{-\gamma} \mathcal{P}(N^{1/\beta} \delta\varphi), \quad (11)$$

assuming the same correlated volume as in Eq. (8). We find a good collapse for $\gamma = 0.27$, see Fig. 3 (b). At φ_J , P vanishes in the thermodynamic limit as $P \sim N^{-\gamma}$ with $\gamma = 0.27$. This exponent relates to the fractal dimension

d_f of \mathbf{e}_i , namely, if $\mathbf{e}_i \cdot \mathbf{e}_i \sim L^{-d_f}$ for $i = 1, \dots, L^{d_f}$, this yields that $P \sim N^{-1+d_f/3}$ [34], leading to

$$d_f = 3(1 - \gamma) = 2.19. \quad (12)$$

Therefore, \mathbf{e}_i has a more compact structure than the bulk $d = 3$. A mean-field theory of the jamming transition predicts that the correlated volume v_{col} and correlation length l_{cor} have the following relation $v_{\text{col}} \sim l_{\text{cor}}^2$ [37, 38]. This may imply that the fractal dimensions is $d_f = 2$, which is close to our estimation Eq. (12).

Interestingly, the similar spatially heterogeneous structures are observed for super-cooled liquids near the glass transition point [39]. For the studies of the glass transition, the degree of spatial heterogeneity is characterized by the so-called non-gaussian parameter [40, 41]. In our setting, an analogous quantity may be written as

$$\alpha_2 = \frac{3 \langle (\delta\mathbf{r}^{\text{NA}})^4 \rangle}{5 \langle (\delta\mathbf{r}^{\text{NA}})^2 \rangle^2} - 1 = \frac{3}{5P} - 1. \quad (13)$$

If the displacements follow the featureless gaussian distribution, one obtains $\alpha_2 = 0$. For the supercooled liquids, α_2 of the displacements during the relaxation time rapidly increases on decreasing the temperature [41, 42]. Similarly, α_2 of our model increases on approaching φ_J , because $P \rightarrow 0$ and $\alpha_2 \propto P^{-1}$. Furthermore, an experimental study for the supercooled colloidal suspensions, which approximately behave as hard spheres [43, 44] and may have the same interaction as our model below jamming, showed that the dynamically correlated regions form a compact cluster of the fractal dimension $d_f = 1.9 \pm 0.4$ [42], reasonably close to our result Eq. (12). Those results suggest the existence of the underlying universality between the dynamics of the athermal system near φ_J and thermal systems near the glass transition point [45, 46].

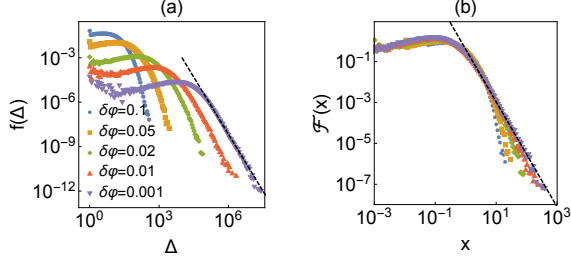


FIG. 4. (a) Distribution of Δ for $N = 4096$ in $d = 3$. Markers are numerical results, while the dashed line denotes the power law $f(\Delta) \sim \Delta^{-2.57}$. (b) Distribution of $x = \Delta/\langle\Delta\rangle$ for the same data. The dashed line denotes $\mathcal{F}(x) \sim x^{-2.57}$.

Distribution function— By using

$$\mathbf{e}_i \cdot \mathbf{e}_i = \Delta_i \frac{3\delta l^2}{\sum_i (\delta \mathbf{r}_i^{\text{NA}})^2}, \quad (14)$$

one can rewrite P as

$$P = \frac{\langle\Delta\rangle^2}{\langle\Delta^2\rangle}, \quad (15)$$

where

$$\langle\Delta^n\rangle = \frac{1}{N} \sum_{i=1}^N \Delta_i^n = \int_0^\infty d\Delta f(\Delta) \Delta^n, \quad (16)$$

with

$$f(\Delta) = \frac{1}{N} \sum_{i=1}^N \delta(\Delta - \Delta_i). \quad (17)$$

Here, we discuss the behavior of P from the perspective of the distribution function $f(\Delta)$ near φ_J . Fig. 4 (a) presents $f(\Delta)$ for several $\delta\varphi$. $f(\Delta)$ has a broader distribution for smaller $\delta\varphi$. For the later convenience, we define a scaled variable $x = \Delta/\langle\Delta\rangle$, and distribution function

$$\mathcal{F}(x) = f(\Delta) \frac{d\Delta}{dx} = \langle\Delta\rangle f(\langle\Delta\rangle x). \quad (18)$$

By definition, $\int dx \mathcal{F}(x) = \int dx \mathcal{F}(x)x = 1$. As shown in Fig. 4 (b), with decreasing $\delta\varphi$, $\mathcal{F}(x)$ develops the power-law tail

$$\lim_{\delta\varphi \rightarrow 0} \mathcal{F}(x) \sim x^{-\zeta} \text{ for } x \gg 1. \quad (19)$$

A similar fat-tail was previously reported for the velocity distribution of sheared driven systems in the quasi-static limit near φ_J [47–49]. Now, we show that the exponent ζ relates to γ in Eq. (11). First, using Eqs. (15), (16), and (18), we get

$$P = \left(\int_0^\infty dx x^2 \mathcal{F}(x) \right)^{-1}. \quad (20)$$

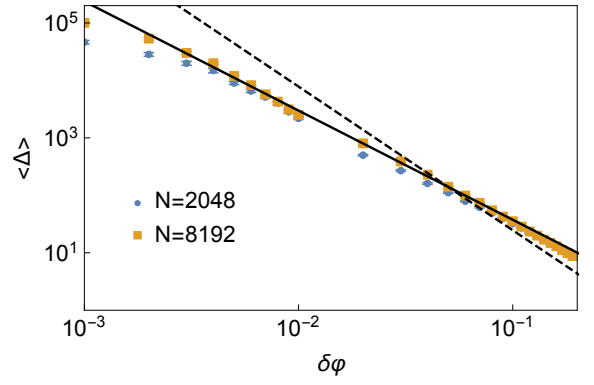


FIG. 5. $\delta\varphi$ dependence of Δ in $d = 2$. Markers denote numerical results. The solid line denotes the power-law fit with $\Delta \sim \delta\varphi^{-1.9}$. For a comparison, we also show the power law in $d = 3$, $\Delta \sim \delta\varphi^{-2.5}$, with the dashed line.

If $\zeta < 3$, the denominator diverges, leading to $P = 0$ at φ_J . For finite N , however, the divergences does not occur as the power law of $\mathcal{F}(x)$ is truncated at finite x_{max} . Using the extreme value statistics, we can calculate x_{max} as

$$\int_{x_{\text{max}}}^\infty \mathcal{F}(x) dx \sim \frac{1}{N} \rightarrow x_{\text{max}} \sim N^{\frac{1}{\zeta-1}}. \quad (21)$$

Then, P for finite N is expressed as

$$P \sim \left(\int_0^{x_{\text{max}}} dx x^2 \mathcal{F}(x) \right)^{-1} \sim N^{-\frac{3-\zeta}{\zeta-1}}. \quad (22)$$

Comparing this with Eq. (11) for $\delta\varphi = 0$, we finally get

$$\zeta = \frac{3+\gamma}{1+\gamma} = 2.57. \quad (23)$$

This is consistent with the assumption $\zeta < 3$ and well agrees with the numerical result, see Fig. 4.

Two dimensional system— Finally, we discuss the dimensional dependence of the critical exponent. We perform numerical simulations in $d = 2$ with the same interaction potential of Eq. (1). Fig. 5 shows the $\delta\varphi$ dependence of $\langle\Delta\rangle$ in $d = 2$, where the numerical data are well fitted with $\langle\Delta\rangle \sim \delta\varphi^{-1.9}$. A similar but a slightly larger exponent $\langle\Delta\rangle \sim \delta\varphi^{-2.2}$ has been reported for a two dimensional system driven by the quasi-static shear [50]. The value of the exponent in $d = 2$ is significantly different from that obtained in $d = 3$. The similar dimensional dependence of the critical exponents was previously reported for the shear viscosity and relaxation time below φ_J [23, 30].

Summary and discussions— In summary, we investigated the statistical properties of the non-affine displacements below the jamming transition point. We showed

that the mean squared of the non-affine displacement diverges toward the jamming transition point. At the jamming transition point, the distribution of the non-affine displacements has a power-law tail, which induces the vanishing behavior of the participation ratio at the jamming transition point in the thermodynamic limit. We also found that the critical exponents in two and three dimensional systems are different, implying that the upper critical dimension is $d_{uc} > 2$, in contrast with above jamming where $d_{uc} \leq 2$.

An interesting question is how the present work relates to the previous works for the shear driven systems. As the shear viscosity η diverges with the same critical exponent as the bulk viscosity η_p near φ_J [51, 52], we consider a system compressed with a finite compression rate $\dot{l} = \dot{L}/L$, instead of the shear driven system. The work done by the imposed compression per time is $p\dot{L}^3 = \eta_p \dot{l}^2 L^3$, where p denotes the pressure, and $\eta_p = p/\dot{l}$ denotes the bulk viscosity. In the quasi-static limit $\dot{l} \rightarrow 0$, this should be balanced with the dissipation $\sum_{i=1}^N (\dot{x}_i^{\text{NA}})^2$, leading to [28, 53]

$$\eta_p \sim \frac{1}{L^3} \sum_{i=1}^N \left(\frac{\dot{x}_i^{\text{NA}}}{\dot{l}} \right)^2 \sim \frac{1}{L^3} \sum_{i=1}^N \left(\frac{\delta x_i^{\text{NA}}}{\delta l} \right)^2 \sim \langle \Delta \rangle. \quad (24)$$

A recent numerical simulation of a sheared suspension in $d = 3$ shows $\eta \sim \eta_p \sim \delta \varphi^{-\beta'}$ with $\beta' = 2.55$ [29], which is close to our result $\langle \Delta \rangle \sim \delta \varphi^{-\beta}$ with $\beta = 2.5$ and thus agrees with the above conjecture. However, a more recent work reported a different value $\beta' = 3.82$ [30]. Further theoretical, numerical, and hopefully experimental studies are necessary to elucidate this point.

We warmly thank A. Ikeda for discussions related to this work. This project has received funding from the JSPS KAKENHI Grant Number JP20J00289.

* hikeda@g.ecc.u-tokyo.ac.jp
† k-hukushima@g.ecc.u-tokyo.ac.jp

[1] M. Van Hecke, *J. Phys. Condens. Matter* **22**, 033101 (2009).
[2] J. Bernal and J. Mason, *Nature* **188**, 910 (1960).
[3] D. J. Durian, *Phys. Rev. Lett.* **75**, 4780 (1995).
[4] G. Katgert and M. van Hecke, *EPL* **92**, 34002 (2010).
[5] Z. Zhang, N. Xu, D. T. Chen, P. Yunker, A. M. Alsayed, K. B. Aptowicz, P. Habdas, A. J. Liu, S. R. Nagel, and A. G. Yodh, *Nature* **459**, 230 (2009).
[6] N. C. Karayiannis, K. Foteinopoulou, and M. Laso, *J. Chem. Phys.* **130**, 164908 (2009).
[7] A. Donev, I. Cisse, D. Sachs, E. A. Variano, F. H. Stillinger, R. Connelly, S. Torquato, and P. M. Chaikin, *Science* **303**, 990 (2004).
[8] A. Jaoshvili, A. Esakia, M. Porro, and P. M. Chaikin, *Phys. Rev. Lett.* **104**, 185501 (2010).
[9] D. Bi, J. Lopez, J. Schwarz, and M. L. Manning, *Nat. Phys.* **11**, 1074 (2015).
[10] M. Delarue, J. Hartung, C. Schreck, P. Gniewek, L. Hu, S. Herminghaus, and O. Hallatschek, *Nat. Phys.* **12**, 762 (2016).
[11] S. Franz and G. Parisi, *J. Phys. A* **49**, 145001 (2016).
[12] S. Franz, S. Hwang, and P. Urbani, *Phys. Rev. Lett.* **123**, 160602 (2019).
[13] C. S. O'Hern, L. E. Silbert, A. J. Liu, and S. R. Nagel, *Phys. Rev. E* **68**, 011306 (2003).
[14] C. P. Goodrich, A. J. Liu, and S. R. Nagel, *Phys. Rev. Lett.* **109**, 095704 (2012).
[15] H. Ikeda, *Phys. Rev. Lett.* **125**, 038001 (2020).
[16] M. Wyart, L. E. Silbert, S. R. Nagel, and T. A. Witten, *Phys. Rev. E* **72**, 051306 (2005).
[17] P. Charbonneau, J. Kurchan, G. Parisi, P. Urbani, and F. Zamponi, *Nat. Commun.* **5**, 1 (2014).
[18] P. Charbonneau, E. I. Corwin, G. Parisi, and F. Zamponi, *Phys. Rev. Lett.* **114**, 125504 (2015).
[19] A. Ikeda, L. Berthier, and G. Biroli, *J. Chem. Phys.* **138**, 12A507 (2013).
[20] J. A. Dronco, M. B. Hastings, C. J. O. Reichhardt, and C. Reichhardt, *Phys. Rev. Lett.* **95**, 088001 (2005).
[21] Q. Liao and N. Xu, *Soft Matter* **14**, 853 (2018).
[22] A. Ikeda, T. Kawasaki, L. Berthier, K. Saitoh, and T. Hatano, *Phys. Rev. Lett.* **124**, 058001 (2020).
[23] Y. Nishikawa, A. Ikeda, and L. Berthier, arXiv preprint arXiv:2007.09418 (2020).
[24] G. Marty and O. Dauchot, *Phys. Rev. Lett.* **94**, 015701 (2005).
[25] P. Olsson and S. Teitel, *Phys. Rev. Lett.* **99**, 178001 (2007).
[26] T. Hatano, *J. Phys. Soc. Jpn.* **77**, 123002 (2008).
[27] C. Heussinger and J.-L. Barrat, *Phys. Rev. Lett.* **102**, 218303 (2009).
[28] E. Lerner, G. Düring, and M. Wyart, *PNAS* **109**, 4798 (2012).
[29] T. Kawasaki, D. Coslovich, A. Ikeda, and L. Berthier, *Phys. Rev. E* **91**, 012203 (2015).
[30] P. Olsson, *Phys. Rev. Lett.* **122**, 108003 (2019).
[31] T. Shen, C. S. O'Hern, and M. D. Shattuck, *Phys. Rev. E* **85**, 011308 (2012).
[32] E. Bitzek, P. Koskinen, F. Gähler, M. Moseler, and P. Gumbsch, *Phys. Rev. Lett.* **97**, 170201 (2006).
[33] R. Yamamoto and A. Onuki, *Phys. Rev. Lett.* **81**, 4915 (1998).
[34] B. Kramer and A. MacKinnon, *Rep. Prog. Phys.* **56**, 1469 (1993).
[35] E. Lerner, G. Düring, and E. Bouchbinder, *Phys. Rev. Lett.* **117**, 035501 (2016).
[36] H. Mizuno, H. Shiba, and A. Ikeda, *PNAS* **114**, E9767 (2017).
[37] L. Yan, E. DeGiuli, and M. Wyart, *EPL* **114**, 26003 (2016).
[38] G. Düring, E. Lerner, and M. Wyart, *Phys. Rev. E* **94**, 022601 (2016).
[39] M. D. Ediger, *Annu. Rev. Phys. Chem.* **51**, 99 (2000).
[40] A. Rahman, *Phys. Rev.* **136**, A405 (1964).
[41] W. Kob and H. C. Andersen, *Phys. Rev. E* **51**, 4626 (1995).
[42] E. R. Weeks, J. C. Crocker, A. C. Levitt, A. Schofield, and D. A. Weitz, *Science* **287**, 627 (2000).
[43] P. N. Pusey and W. Van Megen, *Nature* **320**, 340 (1986).
[44] W. van Megen and S. M. Underwood, *Phys. Rev. E* **49**,

4206 (1994).

[45] G. Marty and O. Dauchot, *Phys. Rev. Lett.* **94**, 015701 (2005).

[46] P. Chaudhuri, L. Berthier, and W. Kob, *Phys. Rev. Lett.* **99**, 060604 (2007).

[47] B. P. Tighe, E. Woldhuis, J. J. C. Remmers, W. van Saarloos, and M. van Hecke, *Phys. Rev. Lett.* **105**, 088303 (2010).

[48] B. Andreotti, J.-L. Barrat, and C. Heussinger, *Phys. Rev. Lett.* **109**, 105901 (2012).

[49] P. Olsson, *Phys. Rev. E* **93**, 042614 (2016).

[50] C. Heussinger, L. Berthier, and J.-L. Barrat, *EPL* **90**, 20005 (2010).

[51] P. Olsson and S. Teitel, *Phys. Rev. Lett.* **109**, 108001 (2012).

[52] D. Vågberg, P. Olsson, and S. Teitel, *Phys. Rev. Lett.* **113**, 148002 (2014).

[53] G. Katgert, B. P. Tighe, and M. van Hecke, *Soft Matter* **9**, 9739 (2013).